

High spin baryon in hot strongly coupled plasma

Miao Li ^{a,b *}, Yang Zhou ^{a,b †} and Push Pu ^{c ‡}

^a *Interdisciplinary Center of Theoretical Studies, University of Science
and Technology of China, Anhui 230026, China*

^b *Institute of Theoretical Physics, Academia Sinica, Beijing 100190, China*

^c *Department of Modern Physics, University of Science and Technology of China,
Auhui 230026, China*

Abstract

We consider a strings-junction holographic model of a probe baryon in the finite-temperature supersymmetric Yang-Mills dual of the AdS-Schwarzschild black hole background. In particular, we investigate the screening length for a high spin baryon composed of rotating N_c heavy quarks. To rotate quarks by finite force, we put a hard infrared cutoff in the bulk and give quarks a finite mass. We find that N_c microscopic strings are embedded reasonably in the bulk geometry when they have finite angular velocity ω , similar to the meson case. By defining the screening length as the critical separation of quarks, we compute the ω dependence of the baryon screening length numerically and obtain a reasonable result which shows that baryons with high spin dissociate more easily. Finally, we discuss the relation between J and E^2 for baryons.

*E-mail: mli@itp.ac.cn

†E-mail: yzhou@itp.ac.cn

‡E-mail: sldvm@mail.ustc.edu.cn

Contents

1	Introduction	1
1.1	Meson in strongly coupled gauge field	2
1.2	Baryon in strongly coupled gauge field	3
2	Baryon configuration	3
3	ω dependence of the screening length	5
4	High spin baryon at nonzero temperature	10
5	Discussion and Conclusion	16

1 Introduction

Recently there has been much interest in studying strongly coupled QCD in terms of AdS/CFT correspondence. The first example of AdS/CFT correspondence is provided by the duality between the classical gravity in $\text{AdS}_5 \times \text{S}^5$ and $\mathcal{N} = 4$ supersymmetric Yang-Mills theory [1]. Quarks can be introduced as fundamental, light ones, which appear in the action. They also can be introduced as external probes, which are often infinitely heavy and not included in the action. In the first case we need introduce the flavor branes, and a background geometry dual to supersymmetric $\text{SU}(N_c)$ Yang-Mills theory with N_f additional hypermultiplets [15]. In this paper we treat the heavy quarks as probes. Since QCD is confining, we always consider a quark and an antiquark together. To measure the interaction potential between them, we choose a physical, gauge invariant object named Wilson loop

$$W[C] = \text{tr} P \exp \int i A_\mu dx^\mu . \quad (1.1)$$

By choosing the contour C as a rectangle with length of \mathcal{T} in the time direction and two sides L in a space direction. When $L \ll \mathcal{T}$, we can extract the potential $V_{q\bar{q}}(L)$ by

$$\langle W(C) \rangle_0 = \exp(-V_{q\bar{q}}(L)\mathcal{T}) . \quad (1.2)$$

In SYM at zero temperature, the potential between probe quark and antiquark separated by L is given by [3, 2]

$$V_{q\bar{q}}(L) = -\frac{4\pi^2}{\Gamma(1/4)^4} \frac{\sqrt{2g_{YM}^2 N}}{L} \quad (1.3)$$

valid in the large N_c and large λ limit. In AdS/CFT framework, we obtain the potential by computing the action of a hanging string with the infinite boundary C of world sheet.

The dual gravity background of SYM gauge theory at a nonzero temperature is an AdS metric with a black hole. The potential between two quarks then becomes [4]

$$V(L, T) \approx \sqrt{\lambda} f(L, T) (L < L_c) \quad V(L, T) \approx \lambda^0 g(L, T) (L > L_c), \quad (1.4)$$

where L_c is a critical separation, at which the qualitative behavior of the interaction potential between a quark and an antiquark changes. Roughly speaking, if $L < L_c$, a quark and an antiquark form a bound state, while if $L > L_c$, they interact weakly relatively. In a hot plasma, the critical length is related to the temperature.

1.1 Meson in strongly coupled gauge field

We consider a quark-antiquark bound state as a meson and define $L_s = L_c$ as the screening length of meson, which is the critical distance between the quark and antiquark. At separation of L_s , the qualitative behavior of interaction potential changes. It is also believed that dissociation happens when the quark-antiquark separation is larger than L_s . For example, once the screening length at a certain temperature is smaller than the radius of meson (such as the J/ψ) in the quark gluon plasma, the quarkonium will dissociate. The dissociation of meson can be used as a signal of the formation of QGP as well as its temperature profile. L_s can be expressed as a decreasing function of temperature and we usually write $L_s = \alpha/T_{diss}$ in a hot plasma, where T_{diss} is the dissociation temperature, and α is a constant determined by the characteristic QCD plasma. Lattice calculations give more details of the static potential between a heavy quark and antiquark in hot QCD [6, 5]. But the potential between moving or rotating quarks is hard to calculate in lattice.

In recent works [7, 8, 20], the screening length of meson is analyzed in the case of a moving quark-antiquark pair. The velocity dependence of the screening length have been calculated¹

$$L_s(v, T) \simeq L_s(0, T)(1 - v^2)^{1/4} \propto \frac{1}{T_{diss}}(1 - v^2)^{1/4}. \quad (1.5)$$

From this equation, we see that the meson can not run too fast in order to avoid dissociation. At a certain temperature, the limiting velocity can be obtained by calculating the dispersion relation of mesons which are described as fluctuation of the flavor brane in the dual gravity background [9, 22].

By studying the spectral function of meson fluctuation on the embedded flavor branes, we can obtain more information about the phase diagram of a strongly coupled gauge theory. The investigation can be extended to more realistic models, such as models with finite chemical potential, isospin density, or the Sakai-Sugimoto model [10]. High spin meson can be described as a rotating string in the gravity background [11, 12, 13].

¹It's pointed out in work [20] that over the entire velocity range $0 \leq v \leq 1$ the behavior of the screening length is actually closer to $(1 - v^2)^{1/3}$ than $(1 - v^2)^{1/4}$ (this can be seen most clearly in Fig.12 in a more recent paper [21]), and it is only in the ultra-relativistic regime $v \rightarrow 1$ that the behavior is in accord with the exponent 1/4 determined analytically in [7].

1.2 Baryon in strongly coupled gauge field

A baryon has a configuration composed of N_c fundamental strings with the same orientation, which begin at the heavy quarks on the boundary and end on the wrapped brane on the junction vertex in the AdS_5 [16]. In the baryon configuration of a very recent work [14], a D5 brane fills S^5 which sits a point in AdS_5 . A simple action of the hanging string and vertex brane was used and the moving velocity dependence of screening length was calculated, which is similar to the meson case.

In this paper, we consider a strings-junction configuration of baryon in the finite temperature supersymmetric Yang-Mills dual of the AdS-Schwarzschild black hole background. In particular, we investigate the screening length for high spin baryons composed of rotating N_c heavy quarks. To rotate the heavy quarks by a finite force, we put a hard infrared cutoff in the bulk and give the quark a finite mass. We find that N_c macroscopic strings are embedded reasonably in the bulk gravity with angular velocity ω , similar to the meson case. By defining the screening length as the critical separation of quarks, we compute the ω dependence of the screening length and find that rotating quarks can dissociate more easily because of the centrifugal force. In section 2, we analyze the baryon configuration in the AdS-Schwarzschild black hole background, and find the strings+brane representation of the high spin baryon in the bulk gravity. In section 3, we find the interesting trajectory of strings in bulk space with angular velocity ω and define the screening length of baryon by using the usual method in a hot plasma. Then we analyze the interaction potential between the quarks and show the critical behavior at the screening length. Finally we get a reasonable ω dependence of baryon screening length. In section 4, we relate the angular momentum J of N_c strings to the high spin of a baryon and defined the energy E and J charge. We pick up some configurations with different ω and analyze the relation between E^2 and J .

2 Baryon configuration

We analyze a baryon composed of N_c heavy probe quarks in the SYM plasma at nonzero temperature. While on the supergravity side, there are N_c fundamental strings with the same orientation, which begin at the heavy quarks on the boundary and end on the junction vertex in the AdS_5 . To give the quarks finite ω , we need to give them a finite mass scale at first, which means that we should put an infrared cutoff in the bulk. We denote the boundary radius r_Λ , then a free quark mass is

$$m_q = \frac{1}{2\pi\alpha'}(r_\Lambda - r_0) . \quad (2.1)$$

where the $\frac{1}{2\pi\alpha'}$ is the string tension and r_0 is the black hole horizon. A free quark can be introduced as a string lying in the radial direction from the boundary to the horizon. Also, an infrared cutoff in the bulk can be realized by introducing a single brane, but for simplicity we just ignore the backreaction and the dynamics of the boundary brane in our paper. The vertex is a D5 brane wrapped on the S^5 which sits at the same point in the AdS_5 . The strings also sit the same point in the S^5 .

The dual background $\text{AdS}_5 \times S^5$ metric with a black hole is:

$$ds^2 = -f(r)dt^2 + \frac{r^2}{R^2}d\vec{x}^2 + \frac{dr^2}{f(r)} + R^2d\Omega_5^2, \quad (2.2)$$

where

$$f(r) = \frac{r^2}{R^2} \left(1 - \frac{r_0^4}{r^4} \right). \quad (2.3)$$

and R is the curvature radius of the AdS metric, r is the coordinate of the 5th dimension of AdS_5 and r_0 is the position of the black hole horizon, $d\Omega_5^2$ is the metric for a unit S_5 . The temperature of the gauge theory is given by the Hawking temperature of the black hole, $T = r_0/(\pi R^2)$. The gauge theory parameters N_c and λ are given by

$$\sqrt{\lambda} = \frac{R^2}{\alpha'}, \quad \frac{\lambda}{N_c} = g_{\text{YM}}^2 = 4\pi g_s, \quad (2.4)$$

where g_s is the string coupling constant and $\frac{1}{2\pi\alpha'}$ is the string tension. Infinite N_c and large λ correspond to large string tension and weak string coupling and thus justify the classical gravity treatment. We define the dimensionless quark mass

$$M_q = \frac{m_q}{T} = \frac{(r_\Lambda - r_0)R^2}{2\alpha'r_0} = \sqrt{\lambda} \frac{r_\Lambda - r_0}{2r_0}. \quad (2.5)$$

When quarks move in a hot plasma, the plasma is like wind if we stand still in the rest frame of quarks. The boosted metric can be used to calculate the velocity dependence of the screening length [14]. In our paper, we consider quarks rotating in the $x_1 - x_2$ plane, the background metric can be written as

$$ds^2 = -f(r)dt^2 + \frac{r^2}{R^2}dx_3^2 + \frac{r^2}{R^2}(d\rho^2 + \rho^2d\theta^2) + \frac{1}{f(r)}dr^2 + R^2d\Omega_5^2 \quad (2.6)$$

where ρ and θ are the coordinates in $x_1 - x_2$ plane.

Now, we consider a rotating strings configuration corresponding a baryon with high spin. It is composed of N_c rotating quarks arranged in a circle on the boundary. For simplicity, we define the same angular velocity of N_c strings as constant ω . The axis lies along radial direction of the AdS and passes through the central of the boundary circle. Then, we parametrize one of N_c strings as

$$\tau = t, \quad \sigma = r, \quad \theta = \omega t, \quad \rho = \rho(r). \quad (2.7)$$

Due to symmetry, N_c strings have the same embedding function $\rho(r)$. The single string Nambu-Goto action is

$$S_{\text{string}} = \frac{1}{2\pi\alpha'} \int d\sigma d\tau \sqrt{-\det[h_{ab}]}, \quad (2.8)$$

where $h_{ab} = g_{\mu\nu} \frac{\partial x^\mu}{\partial \sigma^a} \frac{\partial x^\nu}{\partial \sigma^b}$. We consider zero moving velocity but a finite rotating speed. The v_{x_3} dependence of baryon properties can be read from [14]. The induced metric on the world sheet h_{ab} is time independent, and the action can be written as

$$S_{\text{string}} = \frac{\mathcal{T}}{2\pi\alpha'} \int_{r_e}^{r_\Lambda} dr \sqrt{-\left(\frac{r^2}{R^2}\rho^2\omega^2 - f(r)\right) \left(\frac{1}{f(r)} + \frac{r^2}{R^2}\rho'^2(r)\right)}, \quad (2.9)$$

where \mathcal{T} is the total time. The action for the D5 brane can be written as [14]

$$S_{D5} = \frac{\mathcal{V}(r_e)\mathcal{T}V_5}{(2\pi)^5\alpha'^3}, \quad (2.10)$$

where V_5 is the volume of the compact brane and $\mathcal{V}(r_e) = \sqrt{-g_{00}}$ is the potential for the brane located at $r = r_e$. Since the D5 brane sits at a point in the AdS space, we ignore the ω dependence of the S_{D5} .

The total action of the system is then

$$S_{total} = \sum_{i=1}^{N_c} S_{string}^{(i)} + S_{D5}, \quad (2.11)$$

where we can consider only one typical string to get N_c strings' action for symmetry. We find static baryon configuration through extremizing S_{total} , first with respect to the $\rho(r)$ (we ignore the x_3 and θ for symmetry) that describes the embedding of the N_c strings, and then with respect to $\rho(r_e)$ and r_e , the location of the vertex brane.

Generally, extremizing S_{total} with respect to $\rho(r_e)$ and r_e yields the $x_1 - x_2$ plane and r directions force balance condition(FBC). Since the system is axial symmetric, the position of baryon vertex $\rho(r_e)$ is fixed and treated as the origin in the $x_1 - x_2$ plane. But bulk coordinate r_e is nonzero and believed to be dependent on ω .

As above, we get the radial FBC by extremizing S_{total} with respect to r_e

$$\sum_{i=1}^{N_c} H^{(i)} \Big|_{r_e} = \Sigma, \quad (2.12)$$

where

$$H^{(i)} \equiv \mathcal{L}^{(i)} - \rho'^{(i)} \frac{\partial \mathcal{L}^{(a)}}{\partial \rho'^{(i)}}, \quad (2.13)$$

$$\Sigma \equiv \frac{2\pi\alpha'}{\mathcal{T}} \frac{\partial S_{D5}}{\partial r_e} = \frac{V_5}{(2\pi)^4\alpha'^2} \frac{\partial \mathcal{V}(r_e)}{\partial r_e}, \quad (2.14)$$

In the following section, we will find the shape of the hanging string in the rotating case and the relation between quark separation l_q and r_e change a lot when we increase ω from zero. The ω dependence of embedding function $\rho(r)$ and the spin dependence of baryon screening length will have apparent physical explanation.

3 ω dependence of the screening length

To find the static baryon configuration, we extremize S_{total} with respect to $\rho(r)$ describing trajectories of the N_c strings in AdS. The world sheet Lagrange density with parameters in (2.7) is

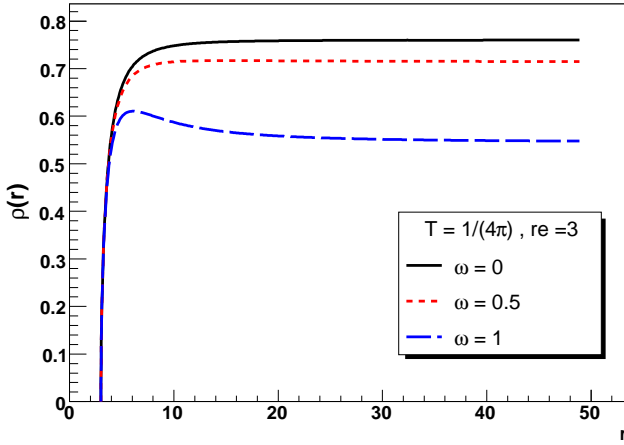


Figure 3: The embedding function $\rho(r)$ at different values of ω with fixed r_e .

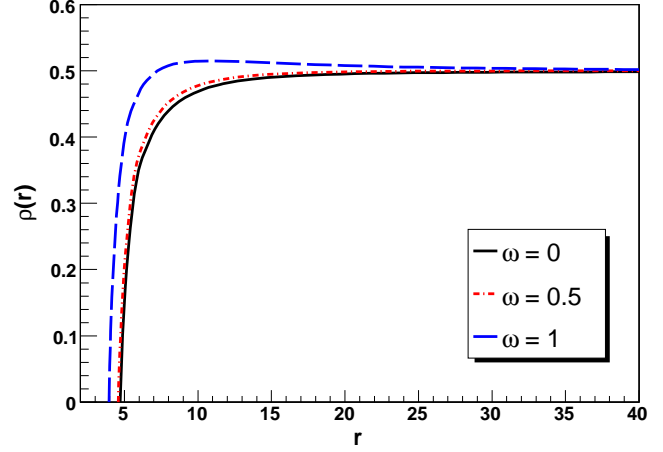


Figure 4: The embedding function $\rho(r)$ at different values of ω with fixed l_q , $r_\Lambda = 100$.

The above equation does not include any unknown function since we choose $r = r_e$. This force balance condition gives

$$\rho'(r_e) = \frac{R}{r_e f(r_e)^{1/2}} \sqrt{\frac{R^2(r_e^4 - r_0^4)r_e^4}{(r_e^4 + r_0^4)^2 A^2} - 1}, \quad (3.5)$$

where

$$A = \frac{1}{N_c} \frac{V_5}{(2\pi)^4 \alpha'^2} \quad (3.6)$$

This equation gives rise to the relation between $\rho'(r_e)$ and r_e . Because $\rho(r)$ depends on $\rho'(r_e)$, we can solve the two equations (3.2) (3.5) numerically together.

Solving equation (3.5), we have one free input value of r_e . It also means that we can input a length of radial trajectory of N_c strings $r_\Lambda - r_e$. When r_e is given, the quark separation on the cutoff brane l_q can be calculated by the solution $\rho(r)$ to

$$l_q = 2 \int_{r_e}^{r_\Lambda} \rho'(r) dr = 2\rho(r_\Lambda). \quad (3.7)$$

When ω increases from 0 to a finite value, the embedding function $\rho(r)$ can be solved, shown in Figure 3. In this figure, we choose the embedding functions of different baryons with the same r_e . Here, by “different”, we mean that the initial separations between quarks and their energy are different even when we have not rotated them. It also means that the interaction potential between quarks are different while $\omega = 0$ for the curves in Figure 3. For baryon of same spin a larger interaction potential also corresponds to a larger boundary quark separation, which will be shown in Figure 9 in the next section. Figure 3 teaches us that the strings warp near the horizon but become straight near the boundary, it's reasonable because the compact D5 brane is like a box which transfers the interaction between the strings. The

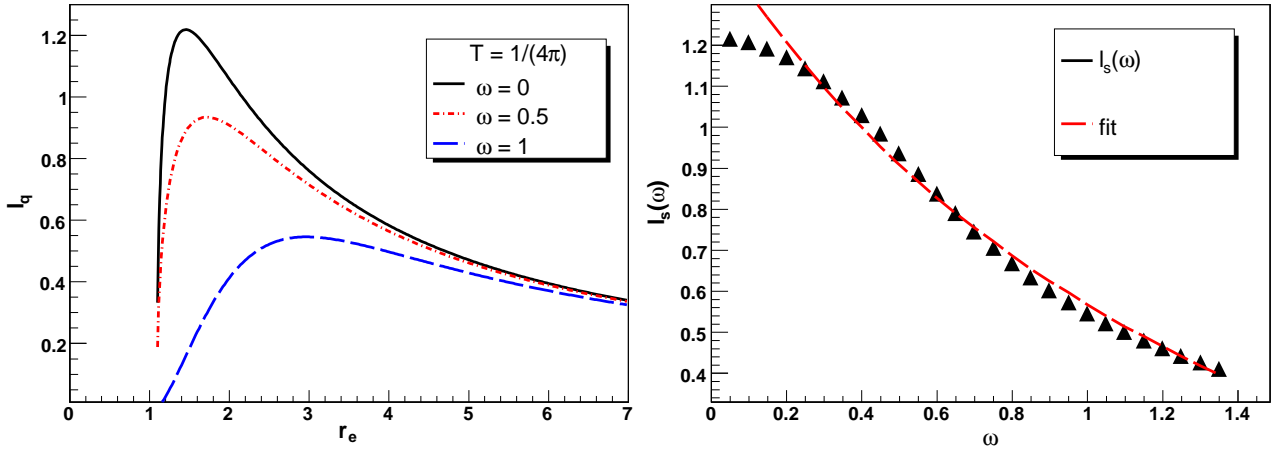


Figure 5: r_e dependence of l_q at different ω . Each Figure 6: ω dependence of the screening length. curve has two branches and we choose the right The fit curve is the modified inverse proportion part as the physical baryons, $r_\Lambda = 100$. function, $r_\Lambda = 100$.

corresponding configuration of the baryon is shown in Figure 2. The tip of the string becomes lower when we increase ω , to guarantee that the speed of the tip is smaller than the speed of light and to make the centrifugal force not too large. Since the bottom part of a hanging string is heavy, at the same centrifugal acceleration, it sticks out in the ρ direction apparently.

If we fix the separation of boundary quarks and stand in the static frame of baryon, the rotating medium will try to separate them and make connecting strings in the bulk longer. We see these solutions in Figure 4. We are interested in the behavior of l_q as r_e changes. For different values of ω , we plot r_e dependence of l_q in Figure 5. In this figure, there is an important phenomenon that l_q becomes large at first and then turns to be smaller, as we increase r_e . Actually, for a given l_q , we get two possible values of r_e from curves in this figure. We consider that the right part of the each curve stands for real baryon states and the left part is unstable and will be thrown away. It is reasonable because in the right part, r_e becomes smaller when l_q becomes larger, which means that a high energy baryon can probe deeper position in the bulk than a low energy baryon if they have same spin. We will see that the energy of a stable baryon with fixed spin must be larger if the average separation between the quarks is larger in the next section. In another view, for baryons of same spin, the only way to have high energy is to keep the quarks with large separation stable. However, we can introduce high spin to revise this relation between l_q and r_e as shown in this figure. High spin helps to weaken the increasing of l_q as r_e becomes smaller. In our classical picture, rotating strings can contribute more energy than unrotating strings.

We define the baryon screening length as the critical quark separation in Figure 5. When ω increases from zero, the screening length seems to decrease as $l_s \propto \frac{1}{\omega}$ in Figure 6. When we fit the curve using

$$l_s = \frac{a}{b\omega + c} - d, \quad (3.8)$$

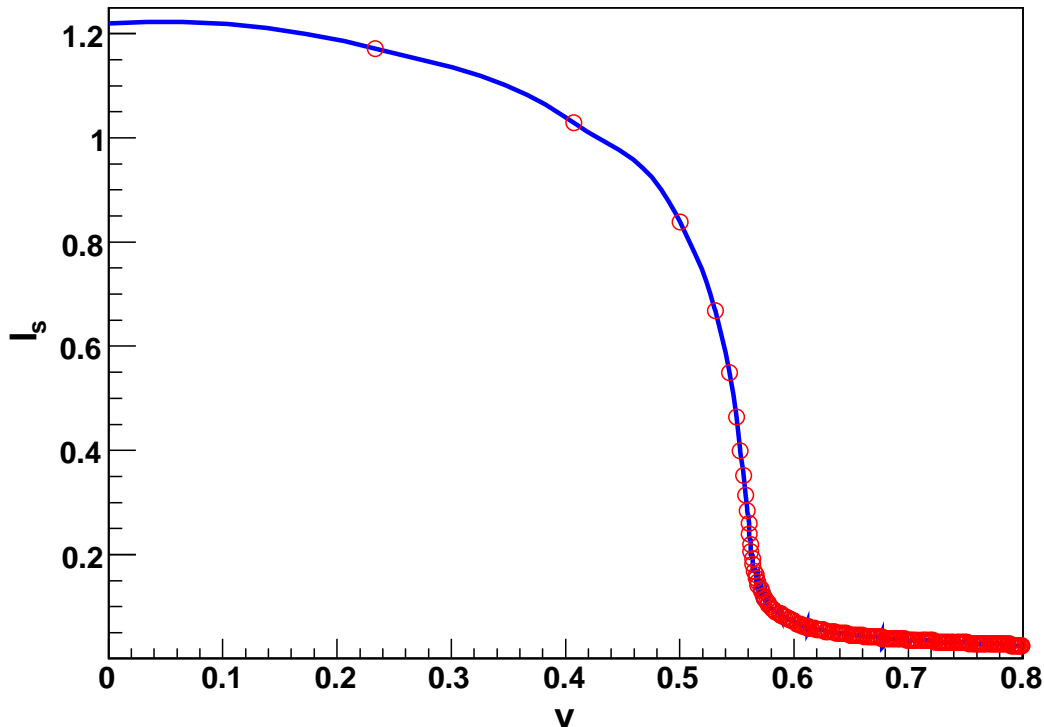


Figure 7: Linear velocity dependence of screening length

we find the best result is

$$l_s = \frac{0.51}{0.14\omega + 0.22} - 0.85. \quad (3.9)$$

We also finished the numerical computation of v dependence of l_s in Figure 7, where v is the linear velocity of quarks, where $v = l_q\omega/2$. When ω is very large, the linear velocity is indeed close to 1. At the same time the quark separation is very small. Our calculation shows that l_s decrease very slowly as the velocity becomes close to 1.² However, we can not find a suitable function like (1.5) to fit the curve. The curve is very different from the usual curve which describes dragging velocity dependence of l_s in (1.5). The main reason we think is that the dragging effect is very different from the rotating effect. Actually, different parts of hanging string have different linear velocities, which is very different from the dragging case. We should note that if we add a drag force in the x_3 direction which is orthogonal to the rotating plane, we may find that v_{x_3} dependence of l_s is similar to (1.5)[11].

In hot plasma, the screening length depends on the temperature directly and it is different for various hadrons. The smaller screening length of a baryon with higher spin makes itself dissociate more easily at a certain temperature in the plasma. The real plasma always becomes

² In our paper, l_s is a parameter which shows how big the baryon can become to keep alive in the plasma. It's different from the "maximum spin size" in [11].

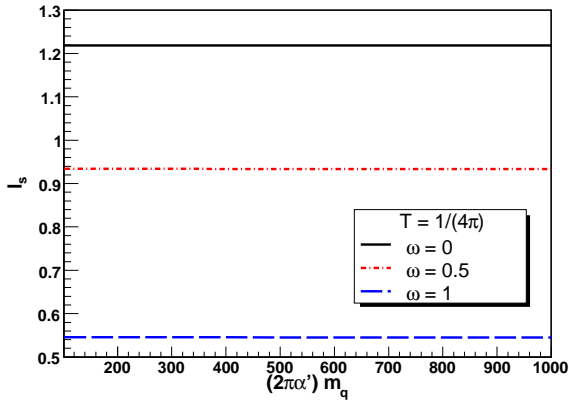


Figure 8: r_Λ dependence of screening length at different values of ω .

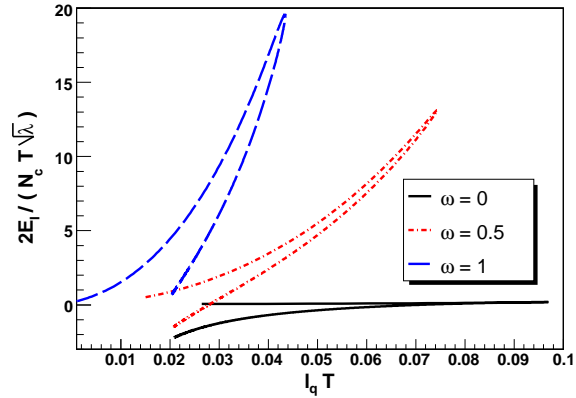


Figure 9: The interaction potential of baryon configuration with a given l_q for several values of the angular velocity ω , $r_\Lambda = 100$. Two branches meet at $l_q = l_s$.

cold very quickly after formation, the baryons with high spin appear later than the low spin baryons.

For simplicity, we ignore the backreaction of the cutoff brane. For different values of m_q , the screening lengths are shown in Figure 8. In this figure, we find that the screening length almost keeps the same value while we choose different cutoffs. It shows that the screening length is a property of the medium, which is a strongly coupled SYM in this case. When we choose a very large cutoff in the bulk, the bulk theory is more like the SYM. Due to conformal invariance of SYM, scale dependence of screening length is negligible.

4 High spin baryon at nonzero temperature

In section 3, we argue that a baryon with high spin can be described by rotating semiclassical strings together with a massive brane. Screening length is considered as the most important signal of quark gluon plasma. Now, we will pay more attention to the properties of the baryon itself. In this section, baryon energy and angular momentum will be defined. More evidence of high spin will be given by the relation of the energy and the angular momentum. We find two branches of $J - E^2$ curves.

Now, we want to give the definition of baryon energy and angular momentum. We write the string Lagrange from the Nambu-Goto action (2.9)

$$L = \frac{1}{2\pi\alpha'} \int_{r_e}^{r_\Lambda} dr \sqrt{-\left(\frac{r^2}{R^2} \rho^2 \omega^2 - f(r)\right) \left(\frac{1}{f(r)} + \frac{r^2}{R^2} \rho'^2(r)\right)}. \quad (4.1)$$

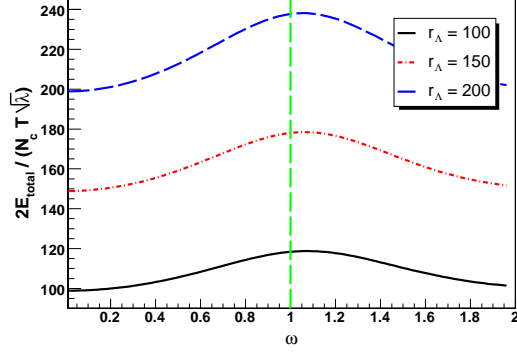


Figure 10: ω dependence of baryon energy with fixed r_e .

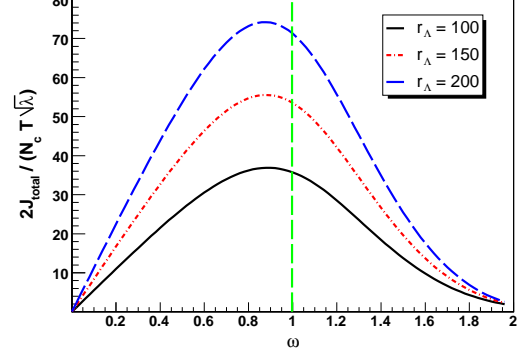


Figure 11: ω dependence of baryon J charge with fixed r_e .

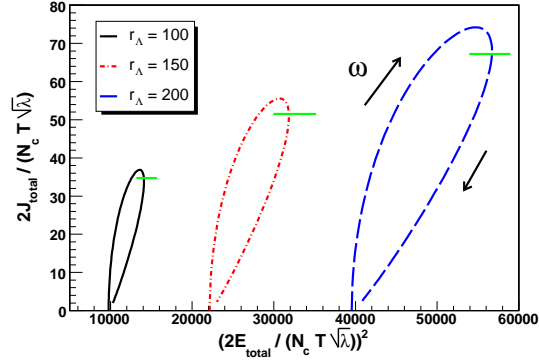
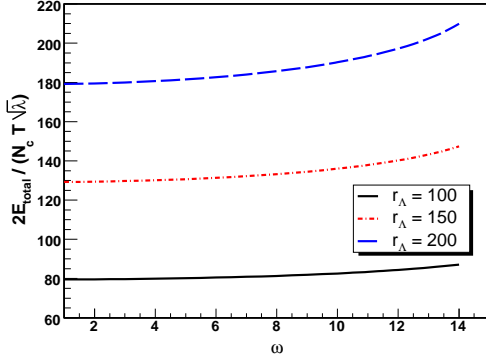


Figure 12: Two branches of $J - E^2$ behavior of Figure 13: ω dependence of baryon energy with fixed l_q on the boundary.



The angular momentum and energy of the string (we choose positive values) are

$$J_{string} = \frac{\partial L}{\partial \omega} = \frac{1}{2\pi\alpha'} \int_{r_e}^{r_\Lambda} dr \frac{\left(\frac{1}{f(r)} + \frac{r^2}{R^2} \rho'^2(r)\right) \left(\frac{r^2}{R^2} \rho^2 \omega\right)}{\sqrt{-\left(\frac{r^2}{R^2} \rho^2 \omega^2 - f(r)\right) \left(\frac{1}{f(r)} + \frac{r^2}{R^2} \rho'^2(r)\right)}}, \quad (4.2)$$

and

$$E_{string} = \omega \frac{\partial L}{\partial \omega} - L = \frac{1}{2\pi\alpha'} \int_{r_e}^{r_\Lambda} dr \frac{\left(\frac{1}{f(r)} + \frac{r^2}{R^2} \rho'^2(r)\right) f(r)}{\sqrt{-\left(\frac{r^2}{R^2} \rho^2 \omega^2 - f(r)\right) \left(\frac{1}{f(r)} + \frac{r^2}{R^2} \rho'^2(r)\right)}}. \quad (4.3)$$

The energy of D5 brane is given by

$$E_{brane} = \frac{\mathcal{V}(r_e) V_5}{(2\pi)^5 \alpha'^3}. \quad (4.4)$$

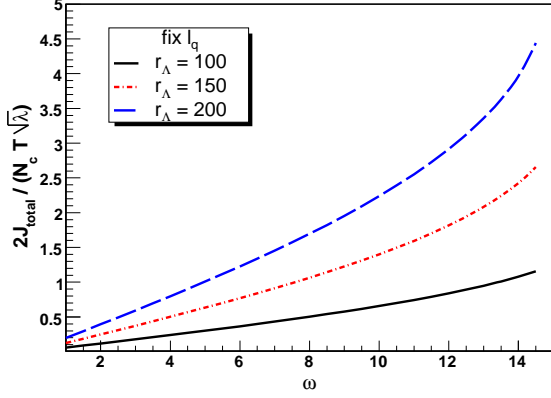


Figure 14: ω dependence of baryon J charge with fixed l_q on the boundary.

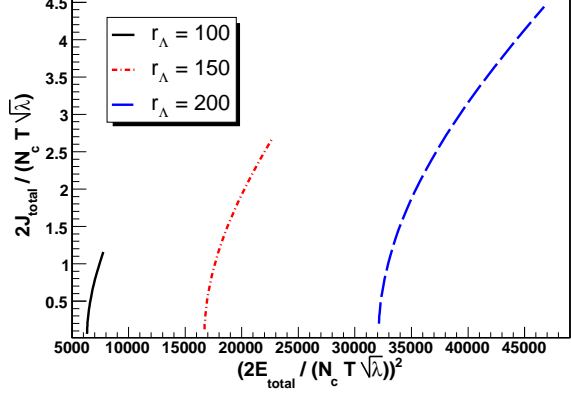


Figure 15: $J - E^2$ behavior of baryon with fixed l_q on the boundary.

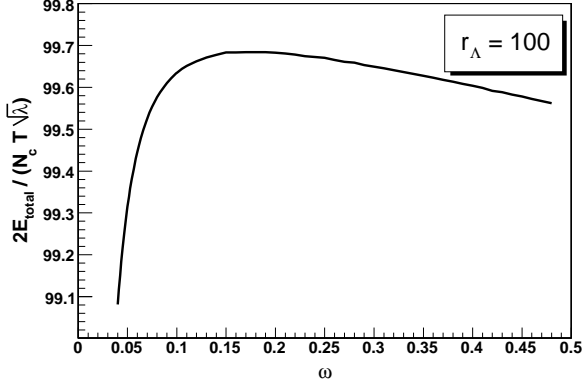


Figure 16: ω dependence of baryon energy with orthogonal boundary condition.

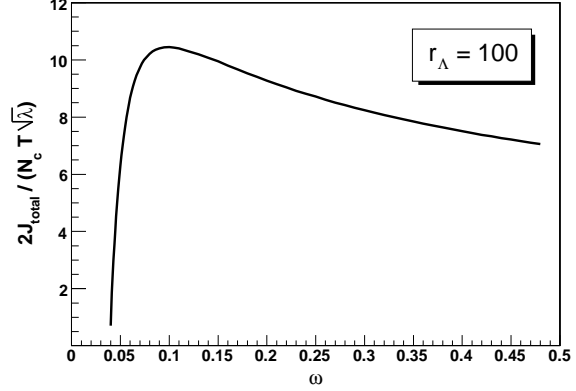


Figure 17: ω dependence of baryon J charge with orthogonal boundary condition .

The total energy and J charge of the baryon can be defined from the bulk strings and compact D5 brane

$$E_{total} = N_c E_{string} + E_{brane}, \quad (4.5)$$

and

$$J_{total} = N_c J_{string} + J_{brane}, \quad (4.6)$$

where E_{string} , J_{string} are string energy and J charge with r_Λ cutoff. Using the above equations (4.2)(4.3)(4.4)(4.5)(4.6), finally we obtain

$$E_{total} = \frac{N_c}{2\pi\alpha'} \int_{r_e}^{r_\Lambda} dr \frac{\left(\frac{1}{f(r)} + \frac{r^2}{R^2} \rho'^2(r) \right) f(r)}{\sqrt{-\left(\frac{r^2}{R^2} \rho^2 \omega^2 - f(r) \right) \left(\frac{1}{f(r)} + \frac{r^2}{R^2} \rho'^2(r) \right)}} + \frac{\mathcal{V}(r_e) V_5}{(2\pi)^5 \alpha'^3}, \quad (4.7)$$

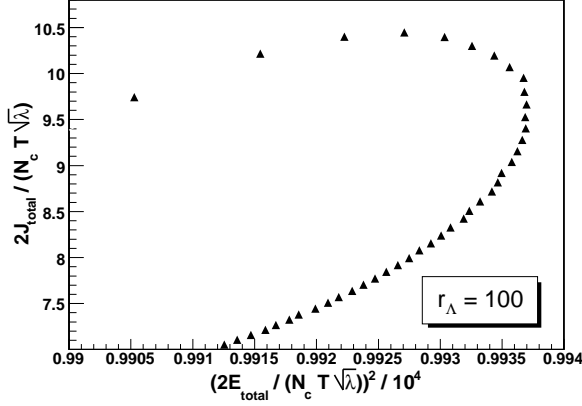


Figure 18: $J - E^2$ behavior of baryon with the orthogonal boundary condition.

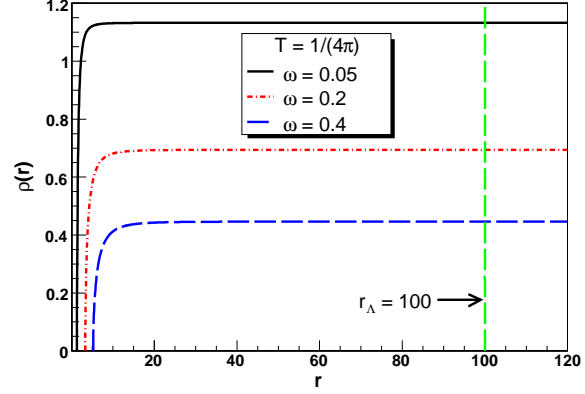


Figure 19: Embedding function with orthogonal boundary condition at different values of ω .

and

$$J_{total} = \frac{N_c}{2\pi\alpha'} \int_{r_e}^{r_\Lambda} dr \frac{\left(\frac{1}{f(r)} + \frac{r^2}{R^2} \rho'^2(r) \right) \left(\frac{r^2}{R^2} \rho^2 \omega \right)}{\sqrt{-\left(\frac{r^2}{R^2} \rho^2 \omega^2 - f(r) \right) \left(\frac{1}{f(r)} + \frac{r^2}{R^2} \rho'^2(r) \right)}} + J_{brane} \quad (4.8)$$

The energy of a hanging string is very large for the mass of free quark, which corresponds to the straight string energy. To define the interaction potential E_I , we need to subtract the N_c free quarks mass³

$$E_q = \frac{N_c}{2\pi\alpha'} \int_{r_0}^{r_\Lambda} dr, \quad (4.9)$$

then the interaction potential can be given

$$E_I = N_c E_{string} - E_q + E_{brane}. \quad (4.10)$$

We find the l_q dependence of the E_I in Figure 9. In this figure, the interaction potential also has a critical behavior at the critical value of l_q ($l_q = L_c$). For the given l_q we choose the low energy as the energy of stable baryon, and the lower energy also corresponds to the larger r_e in Figure 5.

We investigate ω dependence of the baryon energy and J charge with three different conditions. The first one, we fix the r_e . The configurations with different ω are shown in Figure 3. We compute ω dependence of the energy and charge and give the numerical result in figure 10,11⁴. Numerical results about $J_{total} - E_{total}^2$ relation are shown in Figure 12. In figure 10,11,

³At first, we subtract the rotating N_c free quarks mass $E_q = \frac{N_c}{2\pi\alpha'} \int_{r_0}^{r_\Lambda} dr \left(\frac{1}{\sqrt{1-\rho^2(r_\Lambda)\omega^2}} \right)$ and at $\omega \neq 0$ we see a smooth curve along which E and l_q achieve their maximum values at different points in Figure 9(v1 of work [29]). It leads to some puzzles. We thank the editor for pointing out the important question.

⁴We should note that in Figure 10, the left part of each curve divided by the green line corresponds to points with $r_e = 3$ on different curves which include the point ($r_e = 3$) on their right arms in Figure 5. The right arms of curves in Figure 5 are considered as configurations of real baryon probes. (There are same arguments for Figure 11 and 12).

three different curves correspond to three different cutoffs. We can see the ω dependence of E_{total} and J_{total} . We find that as ω increases from zero, the energy and charge become larger at first and then decrease. The curves have highest points both for the energy and charge. We can explain this phenomena. Two main factors of the variance of energy are angular velocity ω and the rotating radius ρ . The former is dominant at first and the latter is dominant when ω is big enough. The same thing happens to the J charge. We find that there are two branches for the $J_{total} - E_{total}^2$ relation of baryons.

The second one, we fix the quark separation l_q on the boundary brane. It implies that we consider the baryons with almost the same size. We compute ω dependence of the energy and charge numerically in Figure 13, 14. We give the $J - E^2$ behavior in Figure 15.

At last, we choose a boundary condition which will be discussed as follow. We want to analyze the boundary condition on the cutoff brane. In section 2, we get the Nambu-Goto action after parameterizing the string world sheet in spacetime:

$$S_{string} = \frac{\mathcal{T}}{2\pi\alpha'} \int_{r_e}^{r_\Lambda} dr \sqrt{-\left(\frac{r^2}{R^2}\rho^2\omega^2 - f(r)\right) \left(\frac{1}{f(r)} + \frac{r^2}{R^2}\rho'^2(r)\right)}. \quad (4.11)$$

Variation of the action gives the boundary term:

$$\frac{\mathcal{T}}{2\pi\alpha'} \frac{\partial \mathcal{L}}{\partial \rho'} \delta \rho \Big|_{r_e}^{r_\Lambda} \quad (4.12)$$

In section 3, we calculate the screening length by considering $\delta\rho(r_\Lambda) = 0$. Because we think that the orbit of the rotating string is exactly a close circle and the radius never changes for the given ω . But $\delta\rho(r_\Lambda) \neq 0$ when we try to change ω . We want to pick up some configurations which can stand for the baryons, with same component quarks but different ω , and analyze ω dependence of the energy and charge. So we choose the boundary condition satisfying $\frac{\partial \mathcal{L}}{\partial \rho'} = 0$, from which we obtain

$$\frac{1}{4} l_q^2 \omega^2 = \left(1 - \frac{r_0^4}{r_\Lambda^4}\right) \quad (4.13)$$

or

$$\rho'(r_\Lambda) = 0. \quad (4.14)$$

We see that the end point of string moves with light speed on the cutoff brane with the first condition (4.13). While the string is orthogonal to the brane with the second condition (4.14).

We now want to give more details about the embedding of the string with angular velocity ω and define properties of baryon with these two boundary conditions. We want to look at the condition (4.13) first. Unfortunately after analyzing a certain $\rho(r)$ with small ω , we can not find a light speed point. Then we look at the condition (4.14). From our numerical result in the section 3, no matter what value of r_e is given, the strings are always orthogonal to the boundary plane in the infinitely point in radial direction. However, for our cutoff r_Λ , we can

only choose a solution satisfying the orthogonal condition in finite point r_Λ , which corresponds to the highest point in Figure 3. Thus we can pick up the string configurations satisfying this orthogonal boundary condition as shown in Figure 19.

All the hanging strings are orthogonal to the cutoff brane. This condition provide us a requirement to pick up one kind of configurations with different spins⁵. Thus we can pick up them and investigate ω dependence of E_{total} and J_{total} . The corresponding embedding functions are shown in Figure 19. The boundary separation $\rho(r_\Lambda)$ becomes small when we increase the ω . Assuming $\omega \sim \rho(r_\Lambda)^n$. From Figure 19, we can set $n = -1.5$. Then we consider a rough and simplest rotating quark picture on the boundary brane. The force balance condition in ρ direction gives

$$\frac{\partial E_I(\rho)}{\partial \rho} = m_q \omega^2 \rho \quad (4.15)$$

where the right part is the centrifugal force. Using $\omega \sim \rho(r_\Lambda)^{-1.5}$, we obtain $E_I \sim \rho^{-1}$. Here, we just ignore the variance of the function $E_I(\rho)$ when ω increases from zero. Let us turn to Figure 9 and look the numerical result. If we fit the curve with $\omega = 0.5$ by using

$$\frac{2E_I}{N_c T \sqrt{\lambda}} = a l_q^c + b, (\rho(r_\Lambda) = l_q) \quad (4.16)$$

we obtain

$$a = -0.060, b = 0.762, c = -1.018 \quad (4.17)$$

while we get

$$a = -0.637, b = 0.949, c = -1.008 \quad (4.18)$$

for the curve with $\omega = 0$. The values of c satisfy $E_I \sim \rho^{-1}$.

We compute the ω dependence of the energy and charge as in Figure 16, 17. And, we compute $J - E^2$ behavior numerically in Figure 18. The curve has two branches and we fit them by using the linear function respectively. We choose the fit function as

$$\frac{2J}{N_c T \sqrt{\lambda}} = a \left(\frac{2E}{N_c T \sqrt{\lambda}} \right)^2 + b, \quad (4.19)$$

then we get

$$a = 601.606, b = -586.255. \quad (4.20)$$

with small ω corresponding to the upper branch and

$$a = 652.6, b = -639.9 \quad (4.21)$$

with large ω corresponding to the lower branch. The value of a can be used to determine the Regge slope, with the coefficients before E and J .

⁵Here, the baryons with orthogonal boundary condition are still unstable if we consider the downward force on the boundary brane. However, this condition can provide us a reasonable requirement for picking up configurations with different ω . The results in Figure 19 satisfy (4.15), which implies that the configurations with this condition do not have other external forces. That is natural and very different from the two former conditions (fixed r_e or l_q).

5 Discussion and Conclusion

In this paper, we calculate the ω dependence of the baryon screening length in hot plasma. We use the strongly coupled SYM gauge theory to describe the quark gluon plasma and consider baryon as a probe. By considering a simple model of baryon in the AdS/CFT frame, we investigate the signatures of baryon probe through the bulk calculation, which are useful to properties of probe of in strongly coupled gauge theory. In particular, we consider baryons with high spin using the rotating strings for the first time, and obtain the ω dependence of the embedding function of hanging strings and screening length. The relation between screening length and spin may be an important experiment signal for the QGP. The energy and charge have been defined for the high spin baryon in our paper. We investigate the $J - E^2$ behavior of baryons, and give the numerical results in three different conditions in our paper. Among them, we argue that these solutions with orthogonal boundary condition are the best candidates for baryons with same component quarks but different spins. The most important is that we obtain two branches of $J - E^2$ behavior. The slope is large for large ω as shown in Figure 18. We ignore the J_{brane} , which means there is no intrinsic spin of D5 brane. These behaviors are probably most important properties of baryons in strongly coupled plasma.

However, in real relativistic heavy ion collisions quark gluon plasma is different from $\mathcal{N} = 4$ SYM. To achieve the goal of understanding phenomena in relativistic heavy ion collisions, conformal invariance is broken via an one-parameter deformation of the AdS black hole dual to the hot $\mathcal{N} = 4$ SYM plasma, and robustness with respect to the introduction of nonconformality of five observables of strongly coupled plasmas that have been calculated in $\mathcal{N} = 4$ SYM theory at nonzero temperature has been investigated [19, 26]. The result shows that, in a toy model, the jet quenching parameter and screening length are affected by the nonconformality at the 20 \sim 30% level or less, but the drag and diffusion coefficients for a slowly moving heavy quark are modified by as much as 80%.

On the other hand, considering the QGP be nonsupersymmetric, we can use other realistic geometry backgrounds. We can compactify a space dimension and give antiperiodic boundary condition for the fermions to break supersymmetry completely. In the baryon model in our paper, the compact brane sits at the same point in the AdS space and has a simple action. Actually the compact brane can be always very heavy and has a nontrivial trajectory in the AdS. For example, in general case the trajectory of the compact brane in the AdS space (including time direction) can be a plane, but not a line.

If we consider different compact D branes, the embedding function of the brane in the bulk can be determined by the DBI action. In this case, the compact brane can be elongated to mimic a string, so the lengths of the string tend to be zero [18, 25, 24, 27]. Properties of baryon will be effected by the brane configuration. Along this way, we can get more interesting properties of the dual baryon model in AdS/CFT and get more informations of the baryon probe in hot plasma.

After this work was finished, there appears very recent work investigating the properties of baryon in strongly coupled gauge field [28].

Acknowledgements

Yang Zhou acknowledges helpful discussions with Tower Wang, Gang Yang, Yushu Song, Chaojun Feng, Yi Wang, Huanxiong Yang and thanks Xian Gao for kind help. Push Pu would like to thank Jian Deng for numerical discussions and Qun Wang for kind help. We thank A. Guijosa for pointing out more references very clearly. We also are very grateful to the editor for kind comments and very important suggestions.

References

- [1] J. M. Maldacena, “The large N limit of superconformal field theories and supergravity,” Adv. Theor. Math. Phys. **2**, 231 (1998) [Int. J. Theor. Phys. **38**, 1113 (1999)] [arXiv:hep-th/9711200]; E. Witten, “Anti-de Sitter space and holography,” Adv. Theor. Math. Phys. **2**, 253 (1998) [arXiv:hep-th/9802150]; S. S. Gubser, I. R. Klebanov and A. M. Polyakov, “Gauge theory correlators from non-critical string theory,” Phys. Lett. B **428**, 105 (1998) [arXiv:hep-th/9802109]; O. Aharony, S. S. Gubser, J. M. Maldacena, H. Ooguri and Y. Oz, “Large N field theories, string theory and gravity,” Phys. Rept. **323**, 183 (2000) [arXiv:hep-th/9905111].
- [2] S. J. Rey and J. T. Yee, “Macroscopic strings as heavy quarks in large N gauge theory and anti-de Sitter supergravity,” Eur. Phys. J. C **22**, 379 (2001) [arXiv:hep-th/9803001].
- [3] J. M. Maldacena, “Wilson loops in large N field theories,” Phys. Rev. Lett. **80**, 4859 (1998) [arXiv:hep-th/9803002].
- [4] S. J. Rey, S. Theisen and J. T. Yee, “Wilson-Polyakov loop at finite temperature in large N gauge theory and anti-de Sitter supergravity,” Nucl. Phys. B **527**, 171 (1998) [arXiv:hep-th/9803135]; A. Brandhuber, N. Itzhaki, J. Sonnenschein and S. Yankielowicz, “Wilson loops in the large N limit at finite temperature,” Phys. Lett. B **434**, 36 (1998) [arXiv:hep-th/9803137]; J. Sonnenschein, “What does the string / gauge correspondence teach us about Wilson loops?,” arXiv:hep-th/0003032.
- [5] O. Kaczmarek and F. Zantow, “Static quark anti-quark interactions in zero and finite temperature QCD. I: Heavy quark free energies, running coupling and quarkonium binding,” Phys. Rev. D **71**, 114510 (2005) [arXiv:hep-lat/0503017].
- [6] O. Kaczmarek, F. Karsch, F. Zantow and P. Petreczky, “Static quark anti-quark free energy and the running coupling at finite temperature,” Phys. Rev. D **70**, 074505 (2004) [Erratum-ibid. D **72**, 059903 (2005)] [arXiv:hep-lat/0406036].
- [7] H. Liu, K. Rajagopal and U. A. Wiedemann, “An AdS/CFT calculation of screening in a hot wind,” Phys. Rev. Lett. **98**, 182301 (2007) [arXiv:hep-ph/0607062].
- [8] H. Liu, K. Rajagopal and U. A. Wiedemann, “Wilson loops in heavy ion collisions and their calculation in AdS/CFT,” JHEP **0703**, 066 (2007) [arXiv:hep-ph/0612168].

- [9] Q. J. Ejaz, T. Faulkner, H. Liu, K. Rajagopal and U. A. Wiedemann, “A limiting velocity for quarkonium propagation in a strongly coupled plasma via AdS/CFT,” arXiv:0712.0590 [hep-th].
- [10] J.Erdmenger, M.Kaminski, F.Rust “Holographic vector mesons from spectral functions at finite baryon or isospin density” arXiv:0710.0334[hep-th] D.Mateos, S.Matsuura, R.C.Myers and R.M.Thomson Holographic phase transitions at finite chemical potential arXiv:0709.1225[hep-th]
- [11] K. Peeters, J. Sonnenschein and M. Zamaklar, “Holographic melting and related properties of mesons in a quark gluon plasma,” Phys. Rev. D **74**, 106008 (2006) [arXiv:hep-th/0606195];
- [12] M. Kruczenski, D. Mateos, R. C. Myers and D. J. Winters, “Meson spectroscopy in AdS/CFT with flavour,” JHEP **0307**, 049 (2003) [arXiv:hep-th/0304032];
- [13] O.Antipin, P.Burikham and J.Li “Effective Quark Antiquark Potential in the Quark Gluon Plasma from Gravity Dual Models” hep-ph/0703105
- [14] C. Athanasiou, H. Liu, K. Rajagopal “Velocity dependence of baryon screening in a hot strongly coupled plasma” arXiv:0801.1117 [hep-th].
- [15] A. Karch and E. Katz, “Adding flavor to AdS/CFT,” JHEP **0206**, 043 (2002) [arXiv:hep-th/0205236]; M. Kruczenski, D. Mateos, R. C. Myers and D. J. Winters, “Meson spectroscopy in AdS/CFT with flavour,” JHEP **0307**, 049 (2003) [arXiv:hep-th/0304032]; J. Babington, J. Erdmenger, N. J. Evans, Z. Guralnik and I. Kirsch, “Chiral symmetry breaking and pions in non-supersymmetric gauge / gravity duals,” Phys. Rev. D **69**, 066007 (2004) [arXiv:hep-th/0306018]; M. Kruczenski, D. Mateos, R. C. Myers and D. J. Winters, “Towards a holographic dual of large- $N(c)$ QCD,” JHEP **0405**, 041 (2004) [arXiv:hep-th/0311270].
- [16] E. Witten, “Baryons and branes in anti de Sitter space,” JHEP **9807**, 006 (1998) [arXiv:hep-th/9805112].
- [17] A. Brandhuber, N. Itzhaki, J. Sonnenschein and S. Yankielowicz, “Baryons from supergravity,” JHEP **9807**, 020 (1998) [arXiv:hep-th/9806158].
- [18] Y. Seo, S.J. Sin, “Baryon Mass in medium with Holographic QCD”, arXiv:0802.0568[hep-th]
- [19] H.Liu, K.Rajapopal and Y.Shi, “Robustness and Infrared Sensitivity of Various Observables in the Application of AdS/CFT to Heavy Ion Collisions”, arXiv:0803.3214[hep-ph]
- [20] M. Chernicoff, J. A. Garcia and A. Guijosa, JHEP **0609**, 068 (2006) [arXiv:hep-th/0607089].
- [21] M. Chernicoff and A. Guijosa, JHEP **0806**, 005 (2008) [arXiv:0803.3070 [hep-th]].

- [22] D. Mateos, R. C. Myers and R. M. Thomson, JHEP **0705**, 067 (2007) [arXiv:hep-th/0701132].
- [23] M. Chernicoff and A. Guijosa, JHEP **0702**, 084 (2007) [arXiv:hep-th/0611155].
- [24] Y. Imamura, Nucl. Phys. B **537**, 184 (1999) [arXiv:hep-th/9807179].
- [25] C. G. . Callan, A. Guijosa and K. G. Savvidy, Nucl. Phys. B **547**, 127 (1999) [arXiv:hep-th/9810092].
- [26] E. Caceres, M. Natsuume and T. Okamura, JHEP **0610**, 011 (2006) [arXiv:hep-th/0607233].
- [27] K. Ghoroku and M. Ishihara, Phys. Rev. D **77**, 086003 (2008) [arXiv:0801.4216 [hep-th]].
- [28] K. Ghoroku, M. Ishihara, A. Nakamura and F. Toyoda, arXiv:0806.0195 [hep-th].
- [29] M. Li, Y. Zhou and P. Pu, arXiv:0805.1611 [hep-th].